Effects of machine errors on the ILC main linac*

WANG Dou(王逗) GAO Jie(高杰)

Institute of High Energy Physics, CAS, Beijing 100049, China

Abstract: For a practical linac, the beam property is affected seriously by any machine imperfections. In this paper, the effects of several main errors in the ILC main linac, such as quadrupole misalignment, magnet strength error and cavity misalignment, were studied by a theoretical method. The tolerance for each error was also obtained. Comparison with the numerical simulation result is made and the agreement is quite good.

Key words: ILC, main linac, machine errors

PACS: 29.20.db **DOI:** 10.1088/1674-1137/35/6/015

1 Introduction

The ILC Main Linacs accelerate the beam from 15 GeV to a maximum energy of 250 GeV over a combined length of 23 km [1]. The linacs utilize L-band (1.3 GHz) superconducting technology, with nine-cell standing-wave niobium cavities operating at an average gradient of 31.5 MV/m in a 2 K superfluid helium bath. The optics consist of simple FODO cells and the beam line components relevant to beam dynamics are accelerating cavities, quadrupole magnets, steering magnets and beam position monitors. Every quadrupole magnet has a steering magnet and a BPM (beam position monitor) attached closely, making a "magnet-BPM package". All beam line components are aligned to the vertically curved line, following the earth's curvature. Table 1 lists the key beam parameters of the main linac.

To achieve the required luminosity in a future e^+ e^- linear collider, one has to produce two colliding beams at the interaction point (IP) with extremely small transverse emittance and precise beam trajectory. Once a beam of this small emittance is produced at the exit of the damping ring, the emittance increases through the long main linac, the preservation of the small emittance and orbit stability becomes important. Many studies have been carried out to try to answer these questions [2–9]. In Ref. [10], we have studied the basic emittance growth in a perfect linac due to the dispersive effect and the wakefield effect. Here, we will go on to study the effects of imperfections that are the main sources of dilution and orbit deviation in a real machine.

Table 1. Nominal beam parameters of the ILC main linacs.

parameter	value
initial beam energy/GeV	15
final beam energy/GeV	250
particles per bunch	2×10^{10}
beam current/mA	9.0
bunch spacing/ns	369
bunch train length/μs	969
number of bunches	2625
pulse repetition rate/Hz	5
initial $\gamma\varepsilon_x$/μm	8.4
final $\gamma\varepsilon_x$/μm	9.4
initial $\gamma\varepsilon_y$/nm	24
final $\gamma\varepsilon_y$/nm	34
σ_z/mm	0.3
initial σ_E=E(%)	1.5
final σ_E =E (e^-, e^+)(%)	0.14, 0.10
beam phase wrt RF crest/(°)	5

In order to solve the orbit deviation resulting from the machine errors, such as quadrupole offset error, magnet strength error, cavity offset and cavity tilt, we consider each kind of error as a random kick perturbation. The error kick transfers from the location S_1 to S_2 by

Received 8 September 2010

* Supported by National Natural Science Foundation of China (10525525, 10775154)

$$\sqrt{\frac{\gamma_1}{\gamma_2}}\begin{pmatrix} \sqrt{\frac{\beta_2}{\beta_1}}(\cos\Delta\varphi+\alpha_1\sin\Delta\varphi) & \sqrt{\beta_1\beta_2}\sin\Delta\varphi \\ -\frac{1+\alpha_1\alpha_2}{\sqrt{\beta_1\beta_2}}\sin\Delta\varphi+\frac{\alpha_1-\alpha_2}{\sqrt{\beta_1\beta_2}}\cos\Delta\varphi & \sqrt{\frac{\beta_1}{\beta_2}}(\cos\Delta\varphi-\alpha_2\sin\Delta\varphi) \end{pmatrix}\begin{pmatrix} 0 \\ \delta \end{pmatrix}, \tag{1}$$

the offset response at S_2 introduced by an upstream kick δ at S_1 is

$$\sqrt{\frac{\gamma_1}{\gamma_2}}\sqrt{\beta_1\beta_2}\sin\Delta\varphi\delta.$$

In this paper, we will use this basic relation to calculate the final rms orbit deviation for the ILC main linac where the beam is accelerated from 15 GeV to 250 GeV. Then the emittance growth can be estimated approximately by (2) [10] when the orbit deviation is very small,

$$\Delta\varepsilon\approx\frac{\langle y_f^2\rangle}{\beta_f}\delta_0^2. \tag{2}$$

2 Quadrupole offset error

The kick given by a quadrupole offset is

$$\delta=K_1L_qy_q, \tag{3}$$

where δ is the kick angle, which comes from the misaligned quadrupole, K_1 and L_q are the normalized strength and the length of the quadrupole, and y_q is the quadrupole's offset error. The kick from the quadrupole will be transported to the end of the linac and yield an orbit deviation. Assuming the misalignment of all of the quadrupoles is completely random, so the rms orbit error at the end of linac will be

$$\begin{aligned}\langle y_f^2\rangle &= \left\langle\left\{\sum_{n=0}^{N_q-1}K_{1n}y_qL_q\sqrt{\beta_n\beta_f}\sqrt{\frac{\gamma_n}{\gamma_f}}\sin\varphi_{nf}\right\}^2\right\rangle \\ &= (\overline{K_1}L_q)^2\langle y_q^2\rangle\frac{\overline{\beta}\beta_f}{\gamma_f}\frac{1}{2}\sum_{n=0}^{N_q-1}\gamma_n \\ &= (\overline{K_1}L_q)^2\langle y_q^2\rangle\frac{\overline{\beta}\beta_f}{\gamma_f}\frac{1}{2}\frac{\gamma_0+\gamma_f}{2}N_q, \end{aligned}\tag{4}$$

where β_n/β_f and γ_n/γ_f are the beta functions and the relative energy factors at the misaligned quadrupole and the end of the linac, $\overline{K_1}$ and $\overline{\beta}$ are the average quadrupole strength and the average beta function, and N_q is the total number of quadrupoles. Further, we can use (2) to get the emittance growth. We can see that the rms final orbit offset is proportional to the integrated quadrupole strength and the misalignment of quadrupoles, and is the square root of the average beta function and the total quadrupole number. If we consider the approximation

$$|K_1L_q|\overline{\beta}\approx\frac{2}{\cos(\varphi_c/2)}$$

Ref. [11], the rms final orbit offset will be proportional to the square root of the integrated quadrupole strength. Thus a weaker focusing lattice is more welcome according to quadrupole misalignment.

For ILC, N_q=278, $\overline{K_1}\approx0.045$ m^{-2}, $\overline{\beta}=80$ m, L_q=0.67 m. So the rms relative vertical orbit offset is

$$\begin{aligned}\sqrt{\frac{\langle y_f^2\rangle}{\beta_f\varepsilon_{f,0}}} &= \sqrt{\frac{\gamma_f\langle y_f^2\rangle}{\beta_f\varepsilon_{N,0}}} \\ &= \sqrt{\frac{\langle y_q^2\rangle}{\varepsilon_{N,0}}(\overline{K_1}L_q)^2\overline{\beta}(\gamma_0+\gamma_f)N_q/4} \\ &= 0.14\Rightarrow\sqrt{\langle y_q^2\rangle}=12\text{ nm}, \end{aligned}\tag{5}$$

where $\varepsilon_{f,0}$ is the nominal emittance at the end of the linac, and $\varepsilon_{N,0}$ is the normalized emittance.

We limit the rms orbit error to $0.14\sigma_0$ because it refers to 3% luminosity reduction. Usually, the theoretical estimation for orbit offset error is more accurate than the analytical emittance growth, because the connection (2) from orbit deviation to emittance growth is a linear approximation [7]. Usually, we should rely on the numerical method to get the precise emittance growth.

To check our theoretical analysis, we used the simulation code SLEPT [12]. SLEPT is a tracking simulation code for high energy linacs, especially for the main linacs of linear colliders, written by Kiyoshi Kubo (KEK). It can be used for ultra-relativistic beam in approximately straight lines, including drift spaces, quadrupole magnets, dipole magnets, accelerating cavities and beam position monitors. Because the relative longitudinal positions of the high energy particles (E >1 GeV) in the bunch are fixed, SLEPT uses slice-macroparticle beam to save the computer disk space and cpu time, in which each bunch is divided into several slices and each slice consists of several macro-particles according to different energy. In fact, there are three other simulation codes ILCv/BMAD, MatLIAR, and PLACET besides SLEPT. Benchmarkings among these four programs

gave good agreement (sub-nano difference for ILC ML even with complex DFS correction). So any of these is fine for our simple tracking without a correction algorithm.

The simulation results for quadrupole position errors are shown in Fig. 1. From Fig. 1, we can see that our theoretical calculation and simulation result agree very well.

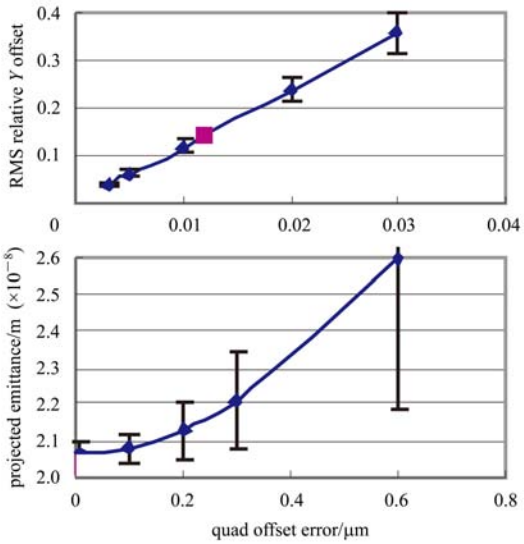

Fig. 1. RMS relative orbit offset and the vertical emitance growth vs. quadrupole offset error (random seeds=50). The diamonds are the simulation results and the square is the theoretical estimation.

3 Magnet strength error

The magnet strength error is important, especially for a curved linac, because there are non-zero designed dipole kicks to steer the beam along the earth curvature and each corrector is combined with the neighboring quadrupole as a package supplied by a shared power source. The magnet strength error can make the final orbit error and emittance grow even without alignment errors.

3.1 Quadrupole strength error

Replacing K_{1n} in (4) by ΔK, we can get the final orbit error at the end of the linac due to the strength errors of the quadrupoles,

$$\langle y_f^2\rangle = \left\langle \left\{ \sum_{n=0}^{N_q-1} \frac{\Delta K}{K_{1n}} K_{1n} y_q L_q \sqrt{\beta_n \beta_f}\sqrt{\frac{\gamma_n}{\gamma_f}}\sin\varphi_{nf} \right\}^2 \right\rangle$$

$$= \left\langle \left(\frac{\Delta K}{K_1}\right)^2 \right\rangle (\overline{K_1} L_q)^2 \langle y_q^2\rangle \frac{\overline{\beta}\beta_f}{\gamma_f}(\gamma_0+\gamma_f)N_q/4. \tag{6}$$

3.2 Corrector strength error

For a quadrupole attached corrector, its kick error will produce a final orbit change. This orbit error can be expressed as

$$\langle y_f^2\rangle = \left\langle \left\{ \sum_{n=0}^{N_q-1} \Delta\theta \sqrt{\beta_n\beta_f}\sqrt{\frac{\gamma_n}{\gamma_f}}\sin\varphi_{nf} \right\}^2 \right\rangle$$

$$= \left\langle \left(\frac{\Delta\theta}{\theta}\right)^2 \right\rangle \overline{\theta}^2 \frac{\overline{\beta}\beta_f}{\gamma_f}(\gamma_0+\gamma_f)N_q/4. \tag{7}$$

Each quadrupole and the attached corrector share a power supply. Using the same relative strength error,

$$\frac{\Delta G}{G} = \frac{\Delta K}{K_1} = \frac{\Delta\theta}{\theta},$$

we can get the collective effects,

$$\frac{\langle y_f^2\rangle}{\beta_f\varepsilon_{f,0}} = \left\langle \left(\frac{\Delta G}{G}\right)^2 \right\rangle (\overline{K_1}L_q)^2\langle y_q^2\rangle \frac{\overline{\beta}}{\varepsilon_{N,0}}(\gamma_0+\gamma_f)N_q/4$$

$$+ \left\langle \left(\frac{\Delta G}{G}\right)^2 \right\rangle \overline{\theta}^2 \frac{\overline{\beta}}{\varepsilon_{N,0}}(\gamma_0+\gamma_f)N_q/4$$

$$= \left\langle \left(\frac{\Delta G}{G}\right)^2 \right\rangle \frac{\overline{\beta}}{\varepsilon_{N,0}}(\gamma_0+\gamma_f)N_q[(\overline{K_1}L_q)^2\langle y_q^2\rangle$$

$$+\overline{\theta}^2]/4, \tag{8}$$

where $\overline{\theta}$ is the average dipole kick of the correctors.

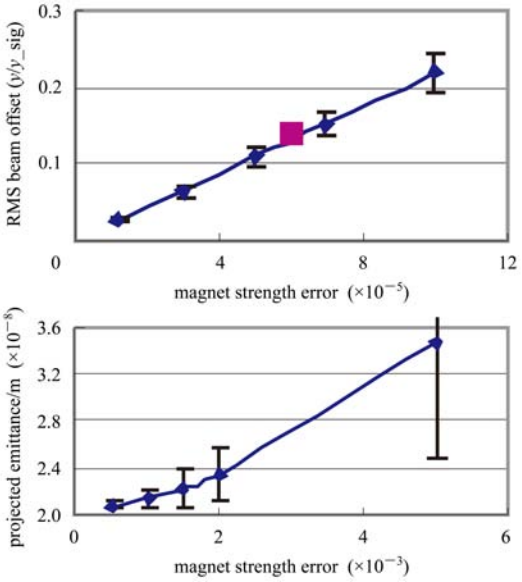

Fig. 2. RMS relative orbit offset and vertical emitance growth vs. magnet strength error without quadrupoles' misalignment (random seeds=50). The diamonds are the simulation results and the square is the theoretical estimation.

To limit the orbit offset to $0.14\sigma_0$, the tolerance for magnet strength error is

$$\sqrt{\frac{\langle y_f^2\rangle}{\beta_f\varepsilon_{f,0}}} = \sqrt{\left\langle\left(\frac{\Delta G}{G}\right)^2\right\rangle\overline{\theta}^2\frac{\overline{\beta}}{\varepsilon_{N,0}}(\gamma_0+\gamma_f)N_q/4}$$

$$= 0.14 \Rightarrow \sqrt{\left(\frac{\Delta G}{G}\right)^2} = 0.006\%, \qquad (9)$$

where we have neglected the quadrupole misalignment. So there is only the correctors' contribution. The simulation results for the magnet strength errors are shown in Fig. 2 [12]. (The quadrupole and its attached corrector are set with the same strength and the quadrupole misalignment is not included.) We can see that the theoretical estimation (9) and the simulation result agree very well. Here, we want to discuss the implications of Eq. (8). If there is no misalignment, the strong focusing lattice is good for the corrector strength error because the rms orbit error is the square root of the average beta function. When the misalignment is included, the additional item about quadrupole strength error will welcome the weaker focusing, just like the discussion of Eq. (4). So the designers have to make a compromise.

4 Cavity misalignment

4.1 Cavity offset

The kick by an offset cavity can be expressed approximately as

$$\delta = \frac{Ne^2W_{\perp1}(z_c)L_c}{m_0\gamma(s)}y_c, \qquad (10)$$

where $W_{\perp1}(z_c)$ is the short-range transverse wake function at the bunch center, L_c is the cavity length, and y_c is the cavity misalignment. Then the rms final orbit change is

$$\langle y_f^2\rangle = \left\langle\left\{\sum_{n=0}^{N_{\rm cavity}-1}\frac{Ne^2W_{\perp1}(z_c)L_c}{m_0\gamma_n}y_c\sqrt{\beta_n\beta_f}\sqrt{\frac{\gamma_n}{\gamma_f}}\sin\varphi_{nf}\right\}^2\right\rangle = \left(\frac{Ne^2W_{\perp1}(z_c)}{m_0}\right)^2L_c\langle y_c^2\rangle\overline{\beta}\beta_f\frac{1}{\gamma_f}\frac{1}{2}\sum_{n=0}^{N_{\rm cavity}-1}\frac{L_c}{\gamma_n}$$

$$\approx \left(\frac{Ne^2W_{\perp1}(z_c)}{m_0}\right)^2L_c\langle y_c^2\rangle\overline{\beta}\beta_f\frac{1}{2\gamma_f}\int_0^L\frac{1}{\gamma(s)}{\rm d}s = \left(\frac{Ne^2W_{\perp1}(z_c)}{m_0}\right)^2L_c\langle y_c^2\rangle\overline{\beta}\beta_f\frac{1}{2\gamma_f}\frac{1}{g}\ln\frac{\gamma_f}{\gamma_0}. \qquad (11)$$

Still, we want to limit the orbit error to $0.14\sigma_0$. The resulting tolerance for random cavity offset is 28 μm compared with 25 μm from our simulation (shown in Fig. 3 [12]). From Eq. (11), we can conclude that a stronger focusing lattice and a higher accelerating gradient will loosen the tolerance for cavity offset error.

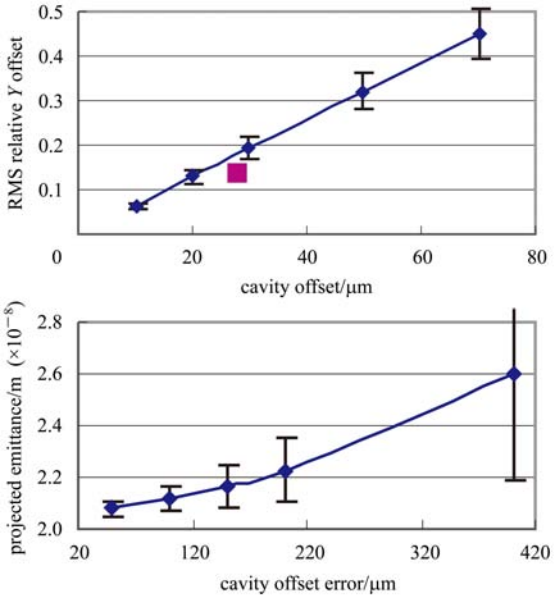

Fig. 3. RMS relative orbit offset and vertical emittrance growth vs. cavity offset error (random seeds=50). The diamonds are the simulation results and the square is the theoretical estimation.

$$\sqrt{\frac{\langle y_f^2\rangle}{\beta_f\varepsilon_{f,0}}} = \sqrt{\frac{\langle y_c^2\rangle}{\varepsilon_{N,0}}\left(\frac{Ne^2W_{\perp1}(z_c)}{m_0}\right)^2\overline{\beta}\frac{L_c}{g}\ln\frac{\gamma_f}{\gamma_0}}$$

$$= 0.14 \Rightarrow \sqrt{\langle y_c^2\rangle} = 28\ \mu{\rm m}. \qquad (12)$$

4.2 Cavity tilt

Besides the cavity offset, cavity tilt can also introduce final orbit error and emittance growth. Here, we just care about the angle error around the x axis because only this angle has a vertical effect. Assuming the cavity is aligned with a tilt angle θ, the resulting kick will be

$$\delta = \frac{eE_{\rm acc}L_c}{2m_0\gamma(s)}\theta = \frac{gL_c}{2\gamma(s)}\theta, \qquad (13)$$

where $E_{\rm acc}$ and g are the accelerating gradient according to the electric field and relative energy factor, respectively.

So,

$$\langle y_f^2\rangle = \left\langle \left\{ \sum_{n=0}^{N_{\rm cavity}-1} \frac{gL_{\rm c}}{2\gamma_n}\theta\sqrt{\beta_n\beta_f}\sqrt{\frac{\gamma_n}{\gamma_f}}\sin\varphi_{nf} \right\}^2 \right\rangle$$
$$= \left(\frac{g}{2}\right)^2 \overline{\beta}\beta_f \frac{L_{\rm c}}{\gamma_f}\frac{1}{2}\langle\theta^2\rangle \sum_{n=0}^{N_{\rm cavity}-1}\frac{L_{\rm c}}{\gamma_n}$$
$$\approx \left(\frac{g}{2}\right)^2 \overline{\beta}\beta_f \frac{L_{\rm c}}{\gamma_f}\frac{1}{2}\langle\theta^2\rangle \int_0^L \frac{1}{\gamma(s)}{\rm d}s$$
$$= \frac{1}{8}g\overline{\beta}\beta_f\frac{L_{\rm c}}{\gamma_f}\langle\theta^2\rangle\ln\frac{\gamma_f}{\gamma_0}. \quad (14)$$

Again, strong focusing is welcome for cavity tilt. But quick acceleration will aggravate the difficulties of mechanical alignment and beam-based alignment due to the cavity tilt influence.

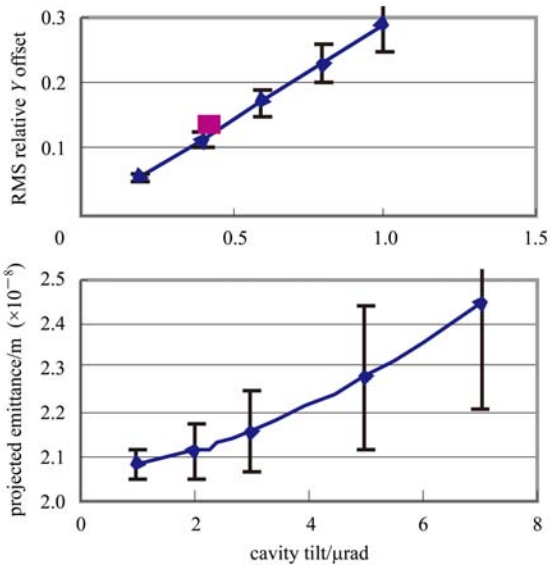

Fig. 4. RMS relative orbit offset and vertical emittance growth vs. cavity tilt error (random seeds=50). The diamonds are the simulation results and the square is the theoretical estimation.

The tolerance for cavity tilt is 420 nrad, which refers to $0.14\sigma_0$ orbit error. Again, it agrees with the simulation result (shown in Fig. 4 [12]).

$$\sqrt{\frac{\langle y_f^2\rangle}{\beta_f\varepsilon_{f,0}}} = \sqrt{\frac{\langle\theta^2\rangle}{\varepsilon_{N,0}}\frac{1}{8}g\overline{\beta}L_{\rm c}\ln\frac{\gamma_f}{\gamma_0}}$$
$$= 0.14 \Rightarrow \sqrt{\langle\theta^2\rangle} = 420\ {\rm nrad}. \quad (15)$$

5 Conclusion

In this paper, the influences of quadrupole misalignment, magnet strength error and cavity misalignment on the final beam orbit error and emittance growth in the ILC main linac were studied. We obtained the explicit formulae to show how the final orbit deviation and the emittance growth are connected to each kind of imperfection and the machine parameters. Also, we gave the tolerance for each fast error (summarized in Table 2), which will provide an essential reference for the design of feedback systems because the fast motion cannot be cured by the trajectory correction technique. The theoretical results have been checked by our simulation studies. In addition, we found that a stronger focusing lattice is helpful to loosen the tolerance of corrector strength error, cavity offset error and cavity tilt error while it is bad for the quadrupole offset and quadrupole strength error. So the final optics should be a balance of all of the imperfections.

Table 2. The tolerance of fast motion refers to 3% IP luminosity loss.

	$0.14\sigma_0$RMS orbit change	achieve in reality
quadrupole offset	12 nm	impossible
magnet strength	6×10^{-5}	easy
cavity offset	28 μm	difficult
cavity tilt	420 nrad	impossible

References

1 ILC Reference Design Report. http://www.linearcollider.org/about/Publications/Reference-Design-Report
2 Chao A, Richter B, YAO C Y. Nucl. Instrum. Methods, 1980, **178**: 1–8
3 Ruth R D. Emittance Preservation in Linear Colliders. Proc. of 1966 US/CERN Part. Acc. School. South Padre Island, TX, 1986
4 Ruth R D. Beam Dynamics in Linear Colliders. Proc. of 1990 Linear Acc. Conf. Albuquerque, NM, 1990
5 Seeman J T. Effects of RF Deflections on Beam Dynamics in Linear Colliders. SLAC-PUB-5069, 1989
6 Raubenhenmer Tor O. The Generation and Acceleration of Low Emittance Flat Beams for Future Linear Colliders. SLAC-387, 1992
7 Raubenhenmer Tor O, Ruth R D. Nucl. Instrum. Methods A, 1991, **302**: 191
8 GAO J. Nucl. Instrum. Methods A, 2000, **441**: 314
9 Amatuni G A, Khachatryan V, Tsakanov V M, Brinkmann R. On the Single Bunch Emittance Preservation in TESLA. TESLA 2001-02, 2001
10 WANG D, GAO J. Single-Bunch Emittance Dilution in the Perfect ILC Main Linac. Chinese Physics C (HEP & NP), 2011, **35**: 296–300
11 Wiedemann H. Scaling of FODO Cell Parameters. SLAC-PEP-Note-39, 1973
12 http: //lcdev. kek. jp/∼kkubo/reports/MainLinac-simulation/SLEPT/SLEPT-index.html